# Analytical Color Gamut Representations*

**Patrick G. Herzog**

*Technical Electronics Institute, Aachen University of Technology, 52056 Aachen, Germany*

A new analytical method represents the surface of a color gamut for a reproduction process based on three or four primary colors by a single, closed expression directly in CIELAB. The method is based on the similarity of a color gamut to a cube (the CMY cube), and this similarity is represented by a *kernel gamut*. The kernel gamut is distorted by distortion and scaling functions in order to match the color gamut. The color gamut is fully represented by the distortion and scaling functions. The total number of their coefficients is below 150 at mean visual errors of below 2.15 $\Delta E_{ab}$ units.

Journal of Imaging Science and Technology 40: 516–521 (1996)

## Introduction

The reproduction of color images is traditionally treated in one of the following ways. In professional color reproduction, much effort is employed to compensate for the different characteristics of input and output devices. Very often scanning and recording of images are included in one single device or single reproduction line in a printing shop, and this is what we call a *closed system* architecture.

Conversely, in commercial desktop applications, colors are represented in a color space (RGB) that is considered to be suited for any kind of color imaging device without any specific calibration or conversion. Consequently, the results of reproduction are extremely poor, and therefore trial-and-error methods of manipulating color are introduced to improve quality. This in turn greatly enlarges the effort, and the quality of professional reproduction is probably never achieved.

The present quality of affordable desktop color devices has reached a rather high level, and hence a better system of color handling is worthwhile. On the other hand, even in the printing industry the creation of an image document is more and more geographically separated from the reproduction, and often, when an image is prepared for reproduction, no knowledge of the kind of printing press is available. This situation represents an *open system*.

Both cases require color management systems that allow device-independent representation of color and that enable the characteristics of an image to be matched to those of a reproduction device in order to match the appearance of the copy to that of the original. Mostly, CIELAB is used as a device-independent color space, but the problem of how to compensate for the mismatch of the ranges of reproducible colors between devices, i.e., their color gamuts, is still under investigation. Apart from very primitive ones, all these methods require knowledge of the surfaces of the color gamuts of both the image and the reproduction device.

This study addresses a compact representation of color gamuts allowing transmission and storage of color gamuts together with images while avoiding a significant increase in the data volume. For this purpose, a new approach is undertaken that is analytical in nature. This approach allows the surface of a color gamut to be represented continuously while avoiding any kind of interpolation.

In the following sections, the basic principles of the new analytical method are explained, followed by a description of its implementation. We continue with a discussion of some results before giving an overview of extensions of the method.

## Basic Principles of the New Method

A typical color reproduction process is controlled by three color-control signals at the input. These may be RGB signals in the case of a CRT monitor or CMY colorant concentrations in the case of a print process. Controlled by the three color signals, colors reproduced at the output can be described in any of the well-known color spaces, e.g., CIELAB, CIEXYZ, or RLAB.[1,2]

In this study, CIELAB is used as an exemplary color space, and a color printer is considered as an example of a reproduction device. In fact, the proposed method is applicable to any existing color-rendering process based on three or four primary colors.

In Fig. 1, the space of color-control signals (cyan, magenta and yellow) of a printer is presented. Each of the three control signals can be modified independently between a minimum and a maximum, i.e., between 0% and 100%. Therefore, all the colors the device can produce are contained in a cube. This cube is called the *CMY cube* or *CMY gamut* in the following discussion. The eight corners of the cube control the full- and zero-tone colors and all the integer mixtures of these colors.

All the colors the printer produces when being controlled by any of the triplets of color control signals make up the *color gamut* of the printer (Fig. 2). This color gamut is the result of the transformation of the CMY cube into the CIELAB space by the printer.

The color gamut normally has a strongly distorted surface, because the relationship between the color space and the space of control signals is strongly nonlinear. However, some significant characteristics of the CMY cube are inherent. Both gamuts have eight corners, 12 edges, and six planes, though edges and planes of the color gamut are somehow distorted. Hence, one gamut can be derived from the other by shifting edges and corners and by distorting edge lines and surfaces by a certain amount. Thus,

Original manuscript received January 16, 1996.

* Presented in part at the 3rd IS&T/SID Color Imaging Conference, November 7–10, 1995, Scottsdale, Arizona.

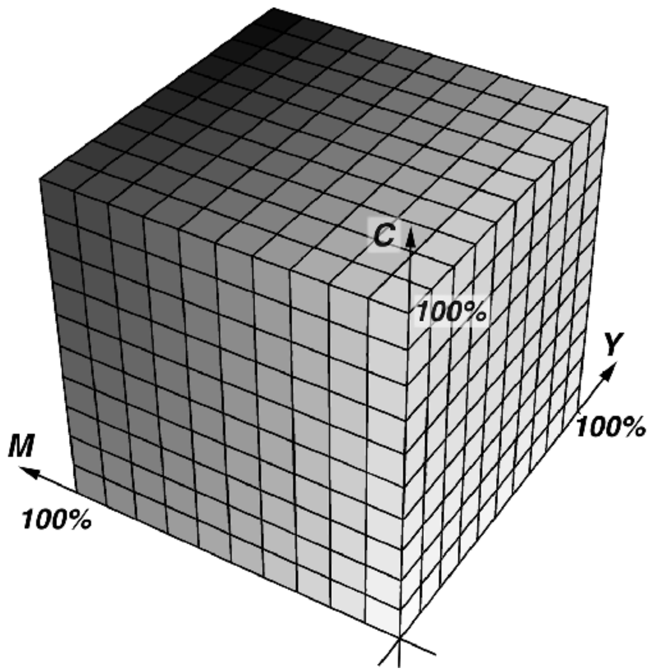


**Figure 1.** The CMY cube of a printer in its space of color control signals.

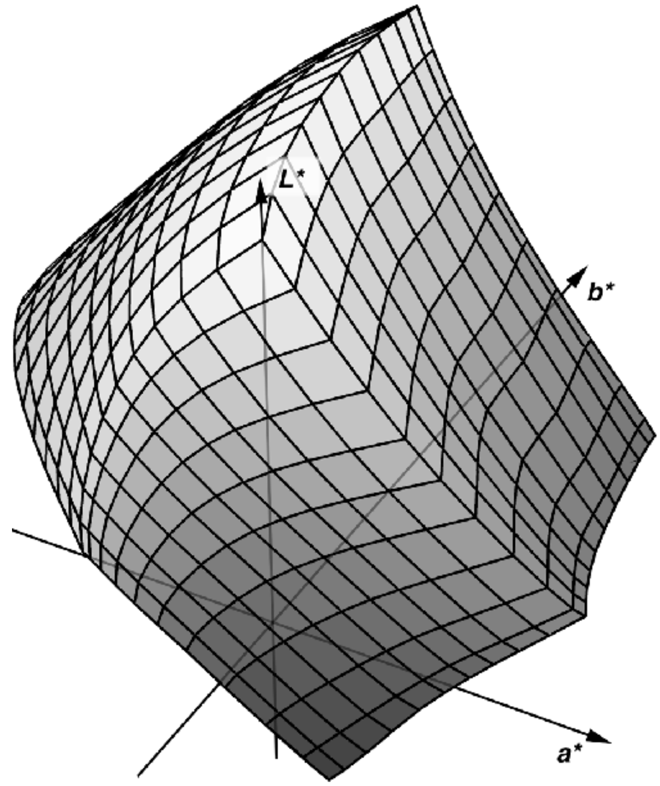


**Figure 2.** The color gamut of a printer in CIELAB.

a color gamut can be described by a transformation into the cube.

So far, the proposed method is based on the similarity of the color gamut and the CMY cube of a printing process. The color gamut is defined by just the measured colors of the test chart, no matter which CMY signals controlled the printer to generate the colors. The method is referred only to the *similarity* of the gamut to a cube, and therefore a general cube in a new, virtual space is considered. Because of the important role of this cube for the method, it is called the *kernel gamut* in the following discussion, and the virtual space is called the *kernel space*.

This cube is now distorted in some way until it matches the color gamut. It appears that the kernel gamut in its virtual space is applicable to the description of the color gamut of any color reproduction process based on three primary colors. Therefore, this method of representing a color gamut by some "tweaking" of the kernel gamut is very general.

The distortion is carried out by analytical functions, mapping the eight corners of the kernel gamut onto the eight corners of the color gamut and, similarly, mapping the edges and planes of the kernel gamut onto the respective edges and planes of the color gamut.

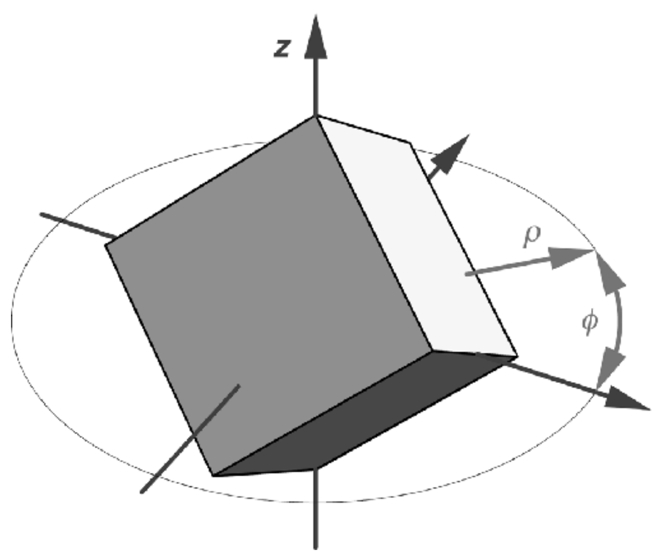


**Figure 3.** The kernel gamut in its mathematical kernel space.

### The Analytical Representation

The kernel gamut used is a unit cube, standing on its vertex, with its center located at the origin of the kernel space. A cylindric coordinate system $z$-$\rho$-$\phi$ is used for the representation (Fig. 3).

The principle of the method is to represent the surface of the color gamut by distorting the well-known kernel gamut. Therefore, a method to describe the surface of the kernel gamut must first be found.

The surface of a three-dimensional object can be expressed mathematically by a function of two variables. Here the surface of the kernel gamut is expressed by the cylindrical radius $\rho$ as a function of $z$ and $\phi$. Figure 4 shows a plot of this function. Because the angle $\phi$ is not defined for points on the $z$ axis, the black point and the white point of the kernel are depicted by the straight lines

$$z = -\frac{\sqrt{3}}{2} \text{ and } z = +\frac{\sqrt{3}}{2},$$

respectively. The remaining six corners are depicted by the six vertices lying in between.

In a similar manner, the surface of the color gamut can be presented two-dimensionally (Fig. 5). Here the cylindrical coordinates have colorimetric meanings: the cylindrical axis is the lightness axis, the cylindrical angle is the hue angle, and the cylindrical radius is chroma.

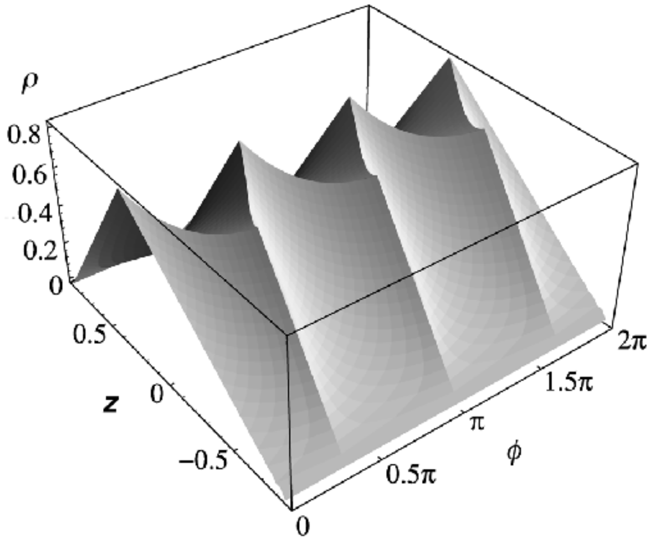


**Figure 4.** The kernel gamut in the two-dimensional presentation.

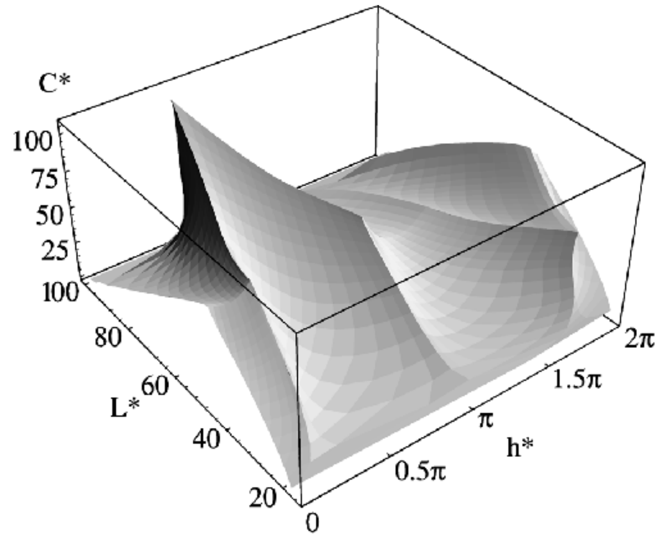


**Figure 5.** The color gamut in the two-dimensional presentation.

Again, the white point and the black point are depicted by the straight lines $L^* = L^*_{\mathrm{white}}$ and $L^* = L^*_{\mathrm{black}}$, respectively (this is true if both are lying on the $L^*$ axis). One recognizes the remaining six corners at lightnesses in between.

**Mathematics.** The surface of the kernel gamut (which is a unit cube) is given in a closed form by the following equation:

$$\rho(z,\phi) = \rho_k(\phi)\,\frac{\dfrac{3}{4} - z\; z_k(\phi) - \dfrac{\sqrt{3}}{2}\left|z - z_k(\phi)\right|}{\dfrac{3}{4} - z_k^2(\phi)}, \qquad (1)$$

with

$$\rho_k(\phi) = \frac{\sqrt{2}}{\left|\sin\phi\right| + \left|\sin\left(\phi - \dfrac{2\pi}{3}\right)\right| + \left|\sin\left(\phi - \dfrac{4\pi}{3}\right)\right|}, \qquad (2)$$

and $z_k(\phi) =$

$$\frac{\left|\cos\phi - \frac{1}{2}\right| - \left|\cos\phi + \frac{1}{2}\right| + \left|\cos\left(\phi + \frac{2\pi}{3}\right) - \frac{1}{2}\right| - \left|\cos\left(\phi + \frac{2\pi}{3}\right) + \frac{1}{2}\right| + \left|\cos\left(\phi + \frac{4\pi}{3}\right) - \frac{1}{2}\right| - \left|\cos\left(\phi + \frac{4\pi}{3}\right) + \frac{1}{2}\right|}{2\left(\left|\sin\phi\right| + \left|\sin\left(\phi - \frac{2\pi}{3}\right)\right| + \left|\sin\left(\phi - \frac{4\pi}{3}\right)\right|\right)}. \qquad (3)$$

Here the absolute values are the means to include the edges and corners into a single, closed expression.

The final chroma function $\hat{C}(L^*,h^*)$ of the color gamut surface is derived from the kernel function $\rho(z, \phi)$ in two steps. In the first step, the kernel function is scaled by multiplication with the scaling function $s(z, \phi)$. This operation transforms $\rho$ into the correct amplitudes of $\hat{C}$, but at coordinates $z$ and $\phi$. In the second step, therefore, the two distortion functions $z_d(L^*,h^*)$ and $\phi_d(L^*,h^*)$ are introduced to move the transformed amplitude values to the right positions in the two-dimensional $(L^*,h^*)$ plane. To improve the performance of the scaling, a further function, $s_a(L^*,h^*)$, is added.

$$\rho_s(z,\phi) = \rho(z,\phi)s(z,\phi), \qquad (4)$$

$$\hat{C}\left(L^*,h^*\right) = \rho_s\left[z_d\left(L^*,h^*\right),\phi_d\left(L^*,h^*\right)\right] + s_a\left(L^*,h^*\right). \qquad (5)$$

In practice, this distortion is approximated by analytical functions composed of simple rational functions, Fourier expansions, etc. The interested reader is referred to the Appendix for more details on the distortion and scaling functions.

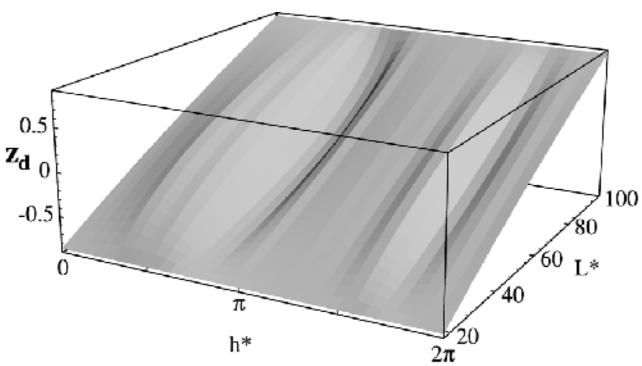


**Figure 6.** Example of a distortion function $z_d(L^*,h^*)$.

**Determination of the Parameters of the Functions.** To determine the parameters of the distortion and scaling functions, a test chart must first be printed and then measured colorimetrically. This is the first procedure to be carried out when a device is characterized. The colors of the test chart subsample the CMY cube of the printer usually equally spaced in three dimensions, and therefore the necessary data for color gamut descriptions are obtained incidentally when a device is calibrated.

In practice, a test chart containing $6 \times 6 \times 6 = 216$ colors was used, but actually only the colors lying on the surface of the color gamut are considered here. Therefore, the number of colors is reduced to 152. The CMY values are of no interest to the method, the measured colors (L*a*b*) themselves being sufficient to define the color gamut. In fact, the colors need not be equally spaced; the data must just be given in a predefined, systematic order. For example, it must be possible to identify the color that was produced by maximum yellow and zero magenta and cyan.

The parameters of the analytical representation are then computed by an iterative algorithm to fit the approximated chroma function $\hat{C}$ to the measured colors. Herewith, some constraints, e.g., monotonicity for some partial functions, must be satisfied. It is beyond the scope of this discussion to describe the algorithm in detail.

**Limitations**. Until now it has been assumed that the white point and the black point lie on the $L^*$ axis. This is true for the white point if colors are referred to the paper white, as is the normal procedure if gamut mapping is to be applied.[3,4] However, in many cases, the black point is located off the gray axis. Then all colors having lightnesses lower than the darkest neutral gray cannot be considered by the method at issue. In practice, however, this loss is not very meaningful, because neutral gray colors should always be mapped to neutrals. Color wedges that include very dark grays and very dark, but more colorful, colors cannot be properly mapped by using color regions that do not include the gray axis. Therefore, one would avoid utilizing these color regions. If the white point must be described with respect to the white of the nonselective diffuser, then all colors lighter than the lightest neutral gray are also cut off.

Another limitation is caused by ambiguities of the gamut surface in terms of the hue angle. Edges and planes of the color gamut are generally more or less curved, both in CIEXYZ and in CIELAB space. CIELAB often increases this effect, because it is known that in CIELAB points of constant hue are not contained on halfplanes of constant hue *angle*. Therefore, because of cavities in the surface, the border of the gamut with respect to the hue angle can be ambiguous. This depends on the location of the $L^*$ axis relative to the gamut.

These ambiguities are very troublesome in practice, because reducing chroma while retaining lightness and hue can lead to out-of-gamut colors. The analytical color gamut representation also cannot handle problems that occur with bright, yellowish colors. Hence, the conclusion is either to cut off these colors that can lead to out-of-gamut colors when reducing chroma or to ignore the fact that colors resulting from reducing only chroma may be out of gamut. Here the author prefers the latter case because it preserves the largest possible volume of the gamut. Out-of-gamut colors then must be mapped onto the nearest possible producible color, a method often implemented in device characterizations. The errors, in practice, are below $\Delta E_{ab} = 3$ and mainly perpendicular to the chroma axis, yielding angular differences of below 2.5 degrees. This is well below the perceptibility threshold of pictorial images of about 5 degrees, as given by Stokes et al.[5,6]

## Results

For the practical application of the method, the required distortion and scaling functions are approximated by combinations of limited polynomials, limited series, etc., to keep the number of parameters as low as possible. Given a pair of values $(L^*,h^*)$, the job of the representation formula is to furnish an optimal representation of the gamut's maximum chroma. Therefore, the visual error is defined solely as the difference between the original and the approximated chroma:

$$\Delta E_{ab} = C^*_{\text{orig}} - \hat{C}. \tag{6}$$

Given an erroneous approximation $\hat{C}$ of the gamut hull for a given pair $(L^*,h^*)$, the nearest point on the actual gamut hull is generally not located in the radial direction. It follows that the distance of the approximated chroma from the gamut hull is actually less than that given by Eq. 6.

The performance of the formula was studied for several output devices (e.g., dye diffusion printer, Cromalin), and we found that the mean visual errors for any device could be kept below 2.15 $\Delta E_{ab}$ units, which is the perceptibility threshold for pictorial images, according to Stokes et al.[5,6]

Because the method is based on the corners and edges of the gamut, these can be represented very accurately. This is important, because these locations contain the most saturated colors the device can produce. In fact, this exactness is given up in favor of a more homogeneous overall error distribution. Therefore, the maximum errors can be located far from edges or near, or on an edge.

In practice, the maximum errors are below 10 $\Delta E_{ab}$ units and are located in the regions of the light yellow edge ([CMY] = [001]) and the dark blue edge ([CMY] = [110]). As mentioned before, the visual error is only an error of chroma, which consequently means an error in the radial direction. If the MacAdam and the Brown–MacAdam ellipses are plotted in the $a^*b^*$ plane, respectively,[7,8] it can be observed that right in these yellow and blue regions the ellipses are strongly nonuniform and that the main axes extend exactly in the direction of the error, i.e., the radial direction. The same is true for the Wyszecky–Fielder ellipses[8] and can also be seen in the CIE 1931 chromaticity diagram.[9] Also, Luo and Rigg[10] show in a compound investigation that ellipses for the yellow and blue centers tend to point along lines of constant dominant wavelength. In other words, the numerical value of the maximum error is relatively high, but the error is expected to be visually much less noticeable. Thus, it can be said that virtually all errors are below the acceptability threshold of normal images, which is specified to be $\Delta E_{ab} = 6$.[6,11]

The necessary number of coefficients of the whole color gamut representation was in the range 100 to 150. There were no investigations on optimal coding, but for simplicity we can assume that 16 bits each will suffice. Therefore, the total data set consists of a number below 300 bytes. It must be pointed out that because the kernel gamut is well defined, the coefficients by themselves represent the whole color gamut.

Figures 6 and 7 show examples of the distortion functions $z_d(L^*,h^*)$ and $\phi_d(L^*,h^*)$, respectively. These functions turn out to be relatively smooth in practical applications. Therefore, relatively simple analytical approximations are possible, yielding low numbers of parameters. We should mention that no kinds of edges are present in these functions. The scaling functions show the same behavior except that they are not monotonic in one direction.

## Extensions of the Analytical Method

**Four-Colorant Print Processes.** Most of the printing processes utilize not three (CMY), but four (CMYK) colorants. The reasons are costs (three color inks are replaced by only one, even cheaper, black ink), enlargement of color gamuts, and the reduction of the amount of wet ink printed on the paper.

With the introduction of a fourth colorant, the problem arises that color is uniquely defined by three terms, but

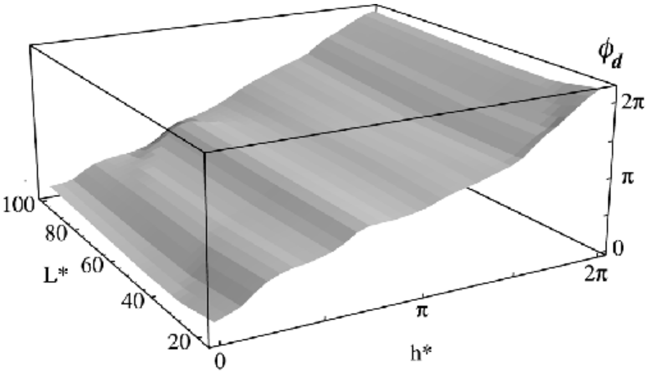


**Figure 7.** Example of a distortion function $\phi_d(L^*,h^*)$.

the space of the color-control signals is four-dimensional. The problem itself will not be addressed here, but if a well-defined algorithm for the separation of three color values into four control signals is assumed, then this algorithm can be considered to be part of the print process, which is then controlled by three signals.

If this separation algorithm (GCR or UCR, for example[12–15]) is well behaved and no jumps and edges are present, then the color gamut of the four-colorant process is very similar to that obtained by using only three inks, though it is widened toward darker colors.

Because only three signals are input to the black box "print process," the analytical representation of color gamuts can be applied to four-colorant processes as well, and the gamut representation is valid for one specified separation algorithm.

**Other Color-Rendering Processes.** The analytical method was developed to give a representation of the color gamuts of color-rendering processes based on three primary colors. The addition of "black" is considered here to be a special case of a three-colorant process, as explained in the preceding section. The method was designed to exhibit a modular structure using a *kernel gamut*. This kernel gamut anticipates the principal characteristics of the process (i.e., edges and corners), so that the distortion and scaling functions can be smooth and well-behaved.

Likewise, it is possible to include other color-rendering processes such as transparency film, six- or seven-colorant processes, etc., into the approach if a particular kernel gamut, specifically designed to represent the basic characteristics of the process, is used. Such processes have not yet been investigated. It seems that the main difficulties will be defining the kernel gamut; the number of parameters is not expected to be higher than for three-colorant processes.

**Extension to the Transformation of Color Spaces.** The analytical distortion and scaling functions, until now considered to be only a means to distort the kernel gamut, can also be considered to represent analytically the transformation between the kernel space and the color space, but this is valid only for the colors contained on the surface of the color or kernel gamut. The extension to the whole space (within the limits of the color gamut) is carried out by defining nested subsurfaces, e.g., surfaces parallel to the outer surface. The analytical correspondences must be determined for any pair of respective subsurfaces of the kernel and the color gamut. Once correct mappings between the corresponding subsurfaces exist, these "submappings" must be combined to form the whole mapping, e.g., by making use of blending functions.

Thus, an analytical formula is given that represents the transformation between the kernel space and the color space in a closed form for all colors lying in the range of reproducible colors of the specific device.

The remaining task is to rotate, translate, and scale the kernel cube by a simple, linear operation to transfer it into the CMY cube. The present result is the analytical description of the transformation from the color-space (CIELAB) into the space of color-control signals (CMY) of the device. Therefore, one can immediately specify the CMY signals that lead to the reproduced color demanded. For more details see Ref. 16.

## Conclusions

The new analytical method described represents the surface of a color gamut by a single, closed expression. Though the method is still under development, it has proved to be very useful, because the errors are within the range of visual perception. Because the representation is very compact, it is well suited to storage or transmission of color gamuts together with images.

Because the method is analytical, no kind of interpolation is required, once the coefficients are determined. The method is applicable to any color space that allows representation by lightness, chroma, and hue.

The new method was demonstrated with a three-colorant print process, but it was shown that processes adding a black colorant can easily be included by the reference to a definite separation algorithm. Moreover, the method is flexible enough to include other color reproduction processes because of its structure based on a *kernel* that can be adjusted to other processes.

As a further application, the method has enough potential to be extended to represent analytically a whole device characterization by giving an analytical transformation from CIELAB to the space of control signals.


**Acknowledgments.** This research was supported by the DFG (Deutsche Forschungsgemeinschaft), Bonn (Germany). The author also wishes to thank Prof. B. Hill for his help in preparing the manuscript.


## Appendix: A Description of the Distortion and Scaling Functions

The distortion and scaling functions described here are the ones temporarily used. Because the method is still under development, they may be changed for the sake of improvement.

**The Scaling Functions.**

$$s(z,\phi) = s(\phi) = s_o + \sum_{n=1}^{N_s} s_{c,n} \cos n\phi + s_{s,n} \sin n\phi, \quad \text{(A1)}$$

$$s_a(L^*,h^*) = s_{a,L^*}(L^*)\left( a_o + \sum_{n=1}^{N} a_{c,n} \cos nh^* + a_{s,n} \sin nh^* \right) \text{(A2)}$$

with

$$s_{a,L^*}(L^*) = 1 - \left( \frac{L^* - \dfrac{L^*_{\max} + L^*_{\min}}{2}}{\dfrac{L^*_{\max} - L^*_{\min}}{2}} \right)^{10}. \quad \text{(A3)}$$

**The Distortion Functions.** The distortion function for the $\phi$ direction is first taken one-dimensionally and computed to yield exact values along the kink-line connecting the six middle vertices (at lightness values between the white point and the black point):

$$\phi_{d,h}(h^*) = h^* + p_0 + \sum_{n=1}^{N_\phi} p_{c,n} \cos nh^* + p_{s,n} \sin nh^*. \quad \text{(A4)}$$

Then it is expanded two dimensionally by introducing a correcting function $\phi_{d,\mathrm{corr}}(L^*,h^*)$ to give also the exact course of the function at the remaining six edges:

$$\begin{aligned}\phi_{d,\mathrm{corr}}(L^* h^*) = {} & \frac{b_1(h^*)}{L^*_{\max} - k_1(h^*)} V(L^* - k_1(h^*)) \\ & + \frac{b_2(h^*)}{k_2(h^*) - L^*_{\max}} V(k_2(h^*) - L^*)\end{aligned} \quad \text{(A5)}$$

with

$$b_i(h^*) = b_{i,0} + b_{i,1} \cos h^* + b_{i,2} \sin h^*, \quad i = 1,2, \quad \text{(A6)}$$

$$k_i(h^*) = k_{i,0} + \sum_{n=1}^{2} k_{i,c,n} \cos nh^* + k_{i,s,n} \sin nh^*, \quad \text{(A7)}$$

$$V(L^*) = L^* + |L^*|. \quad \text{(A8)}$$

Hence, the distortion function $\phi_d(L^*,h^*)$ is

$$\phi_d(L^*,h^*) = \phi_{d,h}(h^*) + \phi_{d,\mathrm{corr}}(L^*,h^*). \quad \text{(A9)}$$

In Fig. 7, a plot of a possible function $\phi_d(L^*,h^*)$ is presented.

The distortion function $z_d$ combines a straight-line part and a fractional rational part for the $L^*$ direction. For the $h^*$ direction, it is modified by a parameter function

$$z_d(L^*,h^*) = \frac{z_{d,0} + z_{h^*}(h^*) + L^*}{z_{d,1} + z_{h^*}(h^*)(1 + L^*)} + z_{d,2} + z_{d,3}L^* \quad \text{(A10)}$$

with

$$z_{h^*}(h^*) = z_0 + \sum_{n=1}^{N_z} z_{c,n} \cos nh^* + z_{s,n} \sin nh^*. \quad \text{(A11)}$$

In Fig. 6, a possible function $z_d(L^*,h^*)$ is plotted.

## References


1. M. D. Fairchild and R. S. Berns, Image color-appearance specification through extension of CIELAB, *Color Res. Appl.* **18**: 178–190 (1993).
2. M. D. Fairchild, Visual evaluation and evolution of the RLAB color space, *Proceedings of the 2nd IS&T/SID Color Imaging Conference: Color Science, Systems and Applications*, Scottsdale, Arizona, 1994, pp 9–13.
3. J. A. Viggiano and C. J. Wang, A comparison of algorithms for mapping color between media of differing luminance ranges, *TAGA Proceedings* (M. Pearson, Ed.) 1992, 959–974.
4. J. Gordon, R. Holub, and R. Poe, On the rendition of unprintable colors, *TAGA Proceedings*, 1987, pp 186–195.
5. M. Stokes, M. D. Fairchild, and R. S. Berns, Precision requirements for digital color reproduction, *ACM Trans. Graphics* **11**(4): 406–422 (Oct. 1992).
6. M. Stokes, M. D. Fairchild, and R. S. Berns, Colorimetrically quantified visual tolerances for pictorial images, *TAGA Proceedings*, (M. Pearson, Ed.) **2**: pp 757–777, (1992).
7. A. R. Robertson, The CIE 1976 color-difference formulae, *Color Res. Appl.* **2**(1): 7–11 (1977).
8. M. Mahy, L. Van Eycken, and A. Oosterlinck, Evaluation of uniform color spaces developed after the adoption of CIELAB and CIELUV, *Color Res. Appl.* **19**(2): 105–121 (1994).
9. J. Romero, E. Hita, and L. Jiménez del Barco, Chromaticity differential thresholds and successive stimuli presentation, *Die Farbe* **32/33**: 264–274 (1985/1986).
10. M. R. Luo and B. Rigg, Chromaticity-discrimination ellipses for surface colours, *Color Res. Appl.* **11**(1): 25–42 (1986).
11. S. Stamm, An investigation of color tolerance, *TAGA Proceedings*, (1981) 156–173.
12. E. Jung, Programmed and complementary color reduction, *TAGA Proceedings*, **36**: pp 135–150, (1984).
13. W. F. Schreiber, A color prepress system using appearance variables, *J. Imaging Technol.* **12**(4): 200–211 (1986).
14. H. R. Kang, Gray component replacement using color mixing models, *Proc. of SPIE*, **2171**: pp 287–296, 1994.
15. P.-C. Hung, A smooth colorimetric calibration technique utilizing the entire color gamut of CMYK printers, *Proc. of SPIE*, **2171**: 275–286, (1994).
16. P. G. Herzog, Analytical color space transformations, *AIC Interim Meeting*, Berlin, September 1995.